

Inhibition of HDAC6 Attenuates Tumor Growth of Non-Small Cell Lung Cancer



Brian Deskin^{*,‡, **}, Qinyan Yin^{*}, Yan Zhuang^{*}, Shigeki Saito^{*}, Bin Shan[†] and Joseph A. Lasky^{*}

^{*}Tulane University Health Sciences Center, Department of Medicine, New Orleans, LA 70112, USA; [†]Washington State University-Spokane, Elson S. Floyd College of Medicine, Department of Biomedical Sciences, Spokane, WA 99210, USA; [‡]Epigenetics & Stem Cell Biology Laboratory, National Institute of Environmental Health Sciences, National Institutes of Health, Research Triangle Park, NC 27709, USA

Abstract

Histone deacetylase 6 (HDAC6) regulates cytoplasmic signaling networks through deacetylation of various cytoplasmic substrates and serves as a key member of the ubiquitin proteasome system (UPS). This study is focused on HDAC6 regulation of the Notch1 receptor that plays a crucial role in tumor growth in NSCLC. A series of cell culture experiments were employed using A549, Lewis lung carcinoma 2 (LL2), and H1299 NSCLC cell lines to investigate HDAC6-mediated regulation of the Notch1 receptor through the UPS. HDAC6 was inhibited with small molecule inhibitors tubacin and ACY1215 *in vitro* and *in vivo*. Inhibition of HDAC6 led to reduced levels of Notch1 receptor in a dose-dependent manner in all three NSCLC cell lines tested. HDAC6 inhibition with ACY1215 led to G2 arrest, increased apoptosis, and increased levels of cleaved PARP1 in A549, LL2, and H1299 cell lines. *In vivo* inhibition of HDAC6 with ACY1215 significantly reduced LL2 tumor growth rate. Our data show that HDAC6 in NSCLC cells supports Notch1 signaling and promotes cell survival and proliferation. Our results support clinical investigation of HDAC6 inhibitors as a potential therapeutic option for treatment of NSCLC patients.

Translational Oncology (2020) 13, 135–10

Introduction

Lung cancer accounts for approximately a quarter of cancer-related mortality in the United States for both men and women [1]. The majority of lung cancers are classified as either small cell or nonsmall cell (NSCLC) and account for 13% and 83% of all lung cancer cases, respectively [2]. The 5-year relative survival rate of NSCLC is only 18% and may in part be related to an advanced stage of disease at the time of diagnosis [3]. The subclassification and stage of NSCLC

dictate the therapeutic intervention strategy [2]. Surgical resection is a common choice of treatment for early stage NSCLC and may be combined with chemotherapy and/or radiation therapy. For advanced stages of NSCLC, patients are usually treated with targeted drugs and chemotherapy [2].

Notch signaling is a requisite feature of the developing lung by directing lineage commitment of progenitor cells in the lung epithelia. Distinct pools of progenitor cells engage Notch signaling to regenerate the lung epithelium after injury and blockade of Notch signaling promotes an alveolar fate [4]. The oncogenic effects of deregulated Notch signaling result in stimulation of NSCLC proliferation, restriction of differentiation, and prevention of apoptotic pathway activation [5]. Notch signaling is deregulated in a variety of tumor types, particularly lung adenocarcinoma [6]. Notch signaling supports tumorigenesis and clinical treatment resistance by inhibition of apoptosis and promotion of proliferation in NSCLC [7].

Histone deacetylase 6 (HDAC6) is a zinc-dependent member of the class IIb HDAC family. The structure of HDAC6 differs from its other

Address all correspondence to: Joseph A. Lasky, 1415 Tulane Avenue, New Orleans, LA 70112, USA. E-mail: jlasky@tulane.edu or Brian Deskin, 665 Huntington Avenue, Building 1-317, Boston, MA 02115, USA. E-mail: bdeskin@hsph.harvard.edu

Received 5 November 2019; Accepted 6 November 2019

© 2019 The Authors. Published by Elsevier Inc. on behalf of Neoplasia Press, Inc. This is an open access article under the CC BY-NC-ND license (<http://creativecommons.org/licenses/by-nc-nd/4.0/>).
1936-5233/19
<https://doi.org/10.1016/j.tranon.2019.11.001>

family members in that it harbors dual deacetylase domains as well as a ubiquitin-binding domain [8]. Although commonly associated with microtubules, HDAC6 plays a key role in receptor trafficking by controlling endocytosis of oncogenic receptors, such as the epidermal growth factor receptor [9]. HDAC6 functions as a cytoskeletal-modulating enzyme through deacetylation of α -tubulin; it also binds ubiquitinated complexes marked for degradation and delivers them to the ubiquitin proteasome system (UPS) [10]. Aggregates of misfolded proteins accumulate and contribute to the pathogenesis of multiple diseases including cancer, neurodegeneration, and age-related disorders [11]. HDAC6 plays a crucial role in maintaining cellular homeostasis by aiding the protein chaperone network to fold misfolded proteins or clearing damaged proteins and misfolded aggregates through the UPS [12,13]. When aggregates of misfolded proteins accumulate, HDAC6 dissociates from the HSP90 chaperone complex to bind ubiquitinated protein aggregates and delivers them to the proteasome [14].

In our previous report, we demonstrated that HDAC6 is required for Notch1 activation by TGF- β 1 in NSCLC cell lines A549 and H1299 [15]. In this report, we demonstrate that HDAC6 is required for Notch1 receptor stabilization in A549, H1299, and Lewis lung carcinoma 2 (LL2) lung cancer cells. We show that Notch1 receptor levels are regulated through the UPS by HDAC6 enzymatic function; inhibition of HDAC6 with small molecules tubacin and ACY1215 reduces total levels of Notch1 receptor. We report that inhibition of HDAC6 induces a G2 cell cycle arrest and induces apoptosis in A549, H1299, and LL2 lung cancer cell lines. Using a syngeneic mouse model of lung carcinoma (LL2), we demonstrate that *in vivo* inhibition of HDAC6 with ACY1215 attenuates LL2 tumor growth. Our results reveal a novel mechanistic role for HDAC6 in the pathobiology of lung cancer and provide rationale for developing therapies targeting HDAC6 as a strategy to treat NSCLC.

Materials and Methods

Reagents and Antibodies

Tubacin and the proteasome inhibitor, MG132, were purchased from Sigma (St. Louis, MO, USA). ACY1215 was purchased from Chemietek (Indianapolis, IN). siRNA targeting human HDAC6 (SI02663808 [siHDAC6_A], SI02757769 [siHDAC6_B], SI03058706 [siHDAC6_C], and SI04438490 [siHDAC6_D]), Notch1 (SI00119035), and AllStars Negative Control siRNA (SI03650318) was purchased from Qiagen (Valencia, CA, USA). Transfections were conducted using the Lipofectamine 2000 Transfection Reagent following the manufacturer's protocol (Invitrogen).

Cell Culture

Human lung adenocarcinoma cell lines A549 and H1299 and the mouse lung carcinoma cell line LL2 were all purchased from the ATCC biological resource center (Manassas, VA). A549 and LL2 cell lines were cultured in Dulbecco's modified Eagle's Medium (Gibco) containing 10% fetal bovine serum (v/v) and 100 μ g/mL penicillin and 100 μ g/mL streptomycin at 37 °C with atmospheric conditions of 95% air and 5% CO₂. The H1299 cell line was cultured in RPMI-1640 (Gibco) containing 10% fetal bovine serum (v/v), 1% L-Glutamine (v/v), 100 μ g/mL penicillin, and 100 μ g/mL streptomycin at 37 °C with atmospheric conditions of 95% air and 5% CO₂. Various concentrations of the HDAC6-specific inhibitors tubacin or ACY1215 were used throughout the study as indicated to assess cell viability, cell cycle progression, and apoptotic markers.

Immunoprecipitation, Immunoblot Analysis, and Antibodies

Whole cell lysates were collected using RIPA containing PMSF and a protease inhibitory cocktail. Electrophoretic grade reagents: MOPS SDS running buffer, NuPAGE Transfer Buffer, and NuPAGE precast gels were obtained from Invitrogen (Carlsbad, CA). Tween 20 was purchased from Fisher Scientific (Waltham, MA). Protease inhibitor cocktail tablets (cOmplete tablets) were purchased from Roche (Nutley, NJ). Protease inhibitor PMSF was purchased from Sigma (St. Louis, MO). Protein concentrations were quantitated using the Bio-Rad DC™ Protein Assay kit (Hercules, CA). Equal amounts of protein from each sample were prepared by resuspension in NuPAGE LDS Sample Buffer followed by heating to 70° for 5 min. Samples were resolved using precast 4–12% Bis-Tris NuPAGE gels (Invitrogen [Carlsbad, CA]) and transferred to a nitrocellulose membrane (Immobilon). Membranes were blocked for 1 h in 5% nonfat dry milk in 1% TBS-T (100 mM Tris, pH 7.6, 0.9% NaCl, and 0.1% Tween 20). Membranes were incubated overnight with appropriate antibodies in 4 °C followed by washing four times with PBS-T. Appropriate secondary antibodies were then added and incubated for 1 h at room temperature followed by washing four times with PBS-T.

Lysates for immunoprecipitation reactions were prepared in RIPA buffer composed of protease inhibitory cocktail (cOmplete tablets) purchased from Roche (Nutley, NJ) (Roche, Indianapolis, IN, USA) and 100 nM PMSF (Sigma, St. Louis, MO, USA). Cells were washed with PBS before lysis with IP buffer. Cell lysates were scraped on ice and passed through a 28-gauge needle five times. The lysates were then boiled for 10 min and allowed to cool to room temperature before centrifugation at 16,000 g for an additional 10 min. The supernatants were transferred to fresh tubes, and protein concentrations were measured using the Bio-Rad DC™ Protein Assay kit. About 2.5 μ g of antiubiquitin antibody (Abcam ab7780, Cambridge, MA, USA) was added to 250 μ g of lysate and incubated overnight on a shaking tumbler at 4 °C. The following day 25 μ L of prewashed protein AG magnetic beads (Pierce, Appleton, WI, USA) was incubated with the lysate-immune complex for 1 h at room temperature on a tumbler. Beads were washed three times with RIPA buffer. After the final wash, beads were collected and residual wash buffer was removed, and 100 μ L of Laemli sample buffer was added to the beads and heated to 70 °C for 10 min. Beads were collected, and the samples were resolved by gel electrophoresis and analyzed by western analysis.

The following rabbit monoclonal antibodies were used for immunoblots (because of the availability of certain antibodies over the course of this study, we have noted the instances when two separate antibodies were used to probe the same target): anti-Notch1 (D6F11) used in Figures 1A, 2A–C, anti-PARP (46D11) used in Figure 5A and C, and anti-GAPDH (14C10) used in Figures 1A and 2A were purchased from Cell Signaling Technologies (Danvers, MA, USA). Rabbit polyclonal anti-HDAC6 (H300), anti-GAPDH (FL-335) used in Figures 1C–E and 3D, and anti-beta actin (C4) were purchased from Santa Cruz (Dallas, TX, USA). Polyclonal antiubiquitin (ab7780) and anti-Notch1 (ab8925) used in Figure 1C–E were purchased from Abcam (Cambridge, MA, USA).

MTT Cell Viability Assay

Viability assays were performed as described [16]. In short, cells were plated at density 2.5×10^3 cells per well in a 96-well plate in

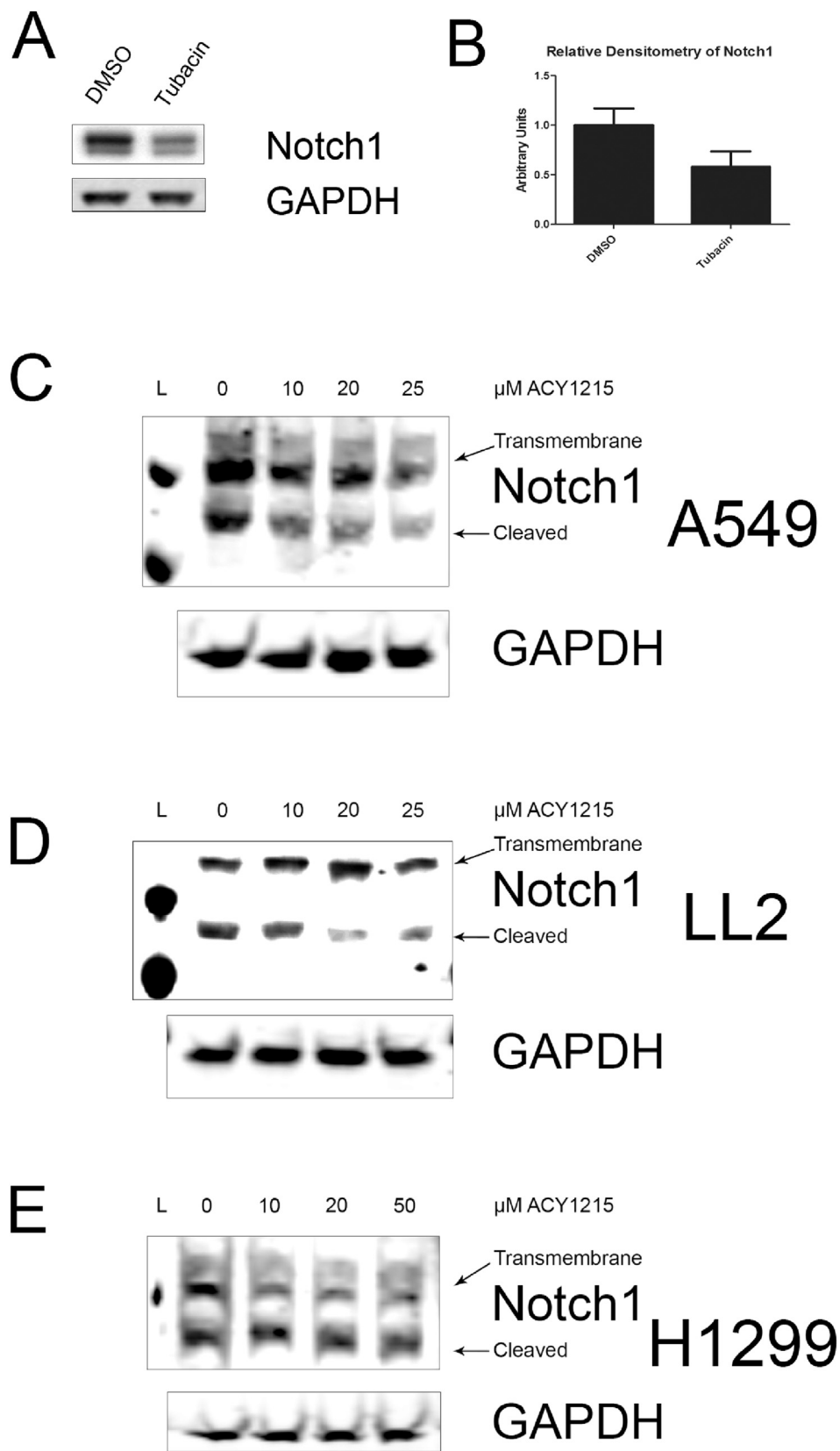


Figure 1. HDAC6 regulates Notch1 receptor levels. (A) Western analysis of A549 cells treated for 24 h with 8 μ M tubacin. (B) Densitometry analysis of panel A Notch1 transmembrane isoform presented as arbitrary units from three independent experiments. (C–E) Western analysis of A549 (D), LL2 (E), and H1299 (F) cells treated for 24 h for the indicated concentration of ACY1215 and analyzed for Notch1 protein levels. Data presented as mean \pm STD of from three replicates.

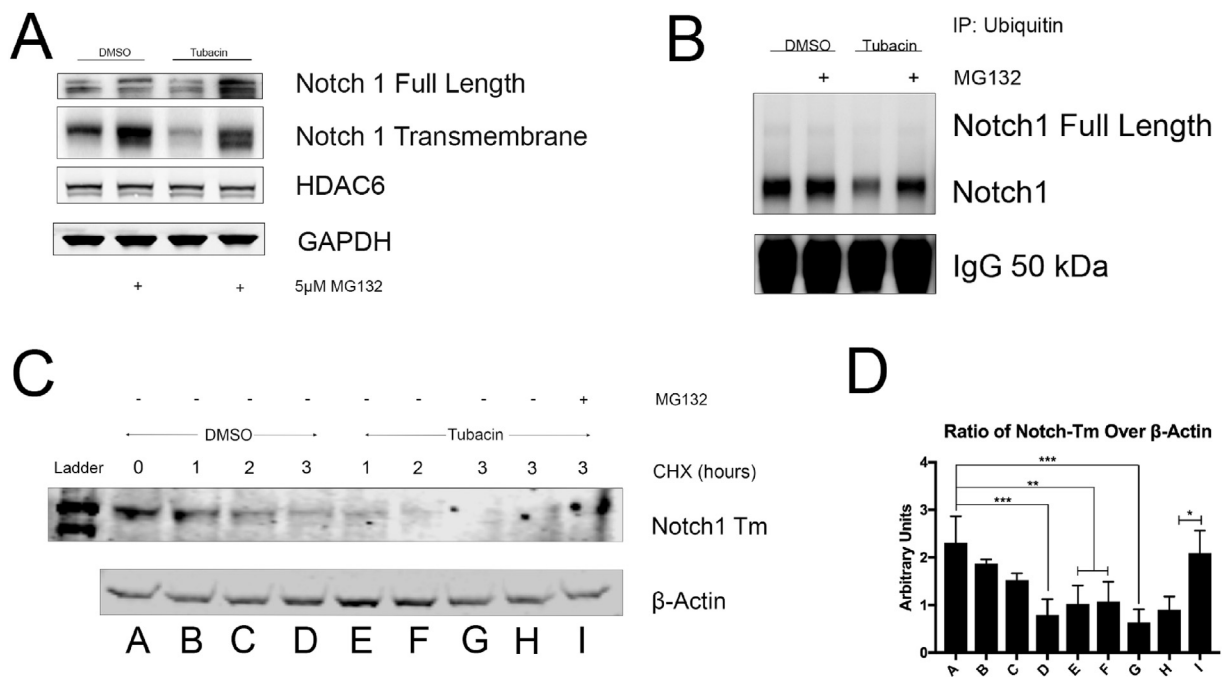


Figure 2. HDAC6 regulation of ubiquitin-mediated degradation of the Notch1 receptor. (A) Western analysis of A549 cells treated with either 8 µM tubacin, 5 µM MG132, or combined treatments for 24 h. (B) Western analysis of immunoprecipitation of ubiquitin in A549 lysates from the same experimental conditions as Panel A. (C) Western analysis of A549 cells cotreated with either 8 µM tubacin alone or in the presence of 100 mg/mL cycloheximide (lanes H and I represent the same experimental conditions as lane G except with an equal volume of DMSO [lane H] or treated with 5 µM MG132 [lane I]). (D) Densitometry analysis of the Notch1 transmembrane (Notch-Tm) isoform from Panel C presented as a ratio of Notch-1 over β-actin and normalized to the control group, lane A. Data presented as mean ± STD of from three independent experiments. ANOVA used to compare treatment groups to lane A; lanes H and I are analyzed by Student's t-test (*p < 0.05; **p < 0.01; ***p < 0.001).

DMEM containing 10% fetal bovine serum (v/v), 100 µg/mL penicillin, and 100 µg/mL streptomycin and allowed to adhere overnight. Cells were then exposed to the inhibitors as indicated for 24 h. In the case of siRNA transfection, cells were transfected the night before the indicated treatments. Following treatment, media was removed and replaced with 100 µL MTT solution (Sigma) diluted in empty DMEM and incubated for 3 h. Cells were lysed with 100 µL MTT solubilization solution (Sigma) and left on a rotary shaker for 30 min. The following day, the absorbance was read with a BioTek Epoch plate reader (BioTek Instruments, Winooski, VT, USA) at 570 nm, with a reference wavelength at 690 nm. Background was adjusted to the absorbance from control wells with no cells plated.

Cell Cycle Analysis

Cells were seeded in 6-well plates and grown overnight to 70% confluency. Cells were treated with inhibitors accordingly for 24 h. After 24 h, cells were trypsinized and pelleted. The cells were washed twice in 1 mL PBS. The cells were then fixed in 70% ethanol for 30 min at 4 °C. After fixation, cells were washed with 9 mLs of 1% FBS-PBS and washed again in 10 mLs of 1% FBS-PBS. A mL of master mix containing 10 µg/mL RNaseA (Qiagen) and 50 µg/mL propidium iodide (Sigma–Aldrich, St. Louis, MO) in 1% FBS-PBS was added to the samples followed by an hour incubation at 37 °C in the dark. Acquisition data were acquired and finalized at 10,000 events using the BD LSRFortessa (BD Biosciences, Franklin Lakes, NJ, USA) running BD FACSDiva software. Cell cycle analysis was modeled using Modfit version 3.2 (Verity Software House, Topsham, ME, USA).

Apoptosis Assay

Cells were seeded in 6-well plates and grown overnight. Cells were treated with inhibitors accordingly for 24 h. After 24 h, cells were trypsinized and pelleted. The eBioscience™ Annexin V Apoptosis Detection Kit APC was used for apoptosis assays (catalog # 88-8007-74, Invitrogen). Acquisition data were acquired and finalized at 10,000 events using the BD LSRFortessa (BD Biosciences, Franklin Lakes, NJ, USA) running BD FACSDiva software.

In Vivo Lung Carcinoma Syngeneic Mouse Model

LL2 cells were transduced with lentiviral particles of LVP324-Luciferase (firefly)-2A-RFP (Amsbio, Cambridge, MA) and kept under puromycin selection (6 µg/mL) for one week. Luciferase activity was confirmed with a luciferase assay (Promega) following the manufacturers' protocol. The transduced LL2 cells (LL2-Luc) were trypsinized and 1 × 10⁷ cells were resuspended in 50 µL Matrigel® (Corning, Bedford, MA). Male C57/Bl6 mice were anaesthetized with 2–4% isoflurane and injected with a 25-gauge needle in the right hind caudal thigh muscle with the LL2–Luc–Matrigel cell suspension. Tumor growth was monitored weekly in the living animals via bioluminescent imaging using the IVIS Lumina XR Imaging System (PerkinElmer, Waltham, MA). Ten minutes before bioluminescent imaging *in vivo* mice were anaesthetized with 2–4% isoflurane and injected intraperitoneally with 200 mg/kg D-Luciferin (PerkinElmer, Waltham, MA) in 1 × PBS. One week after LL2 tumor implantation, ACY1215 treatment was initiated *in vivo*. In short, 8 mice per each group were injected 5 days consecutively

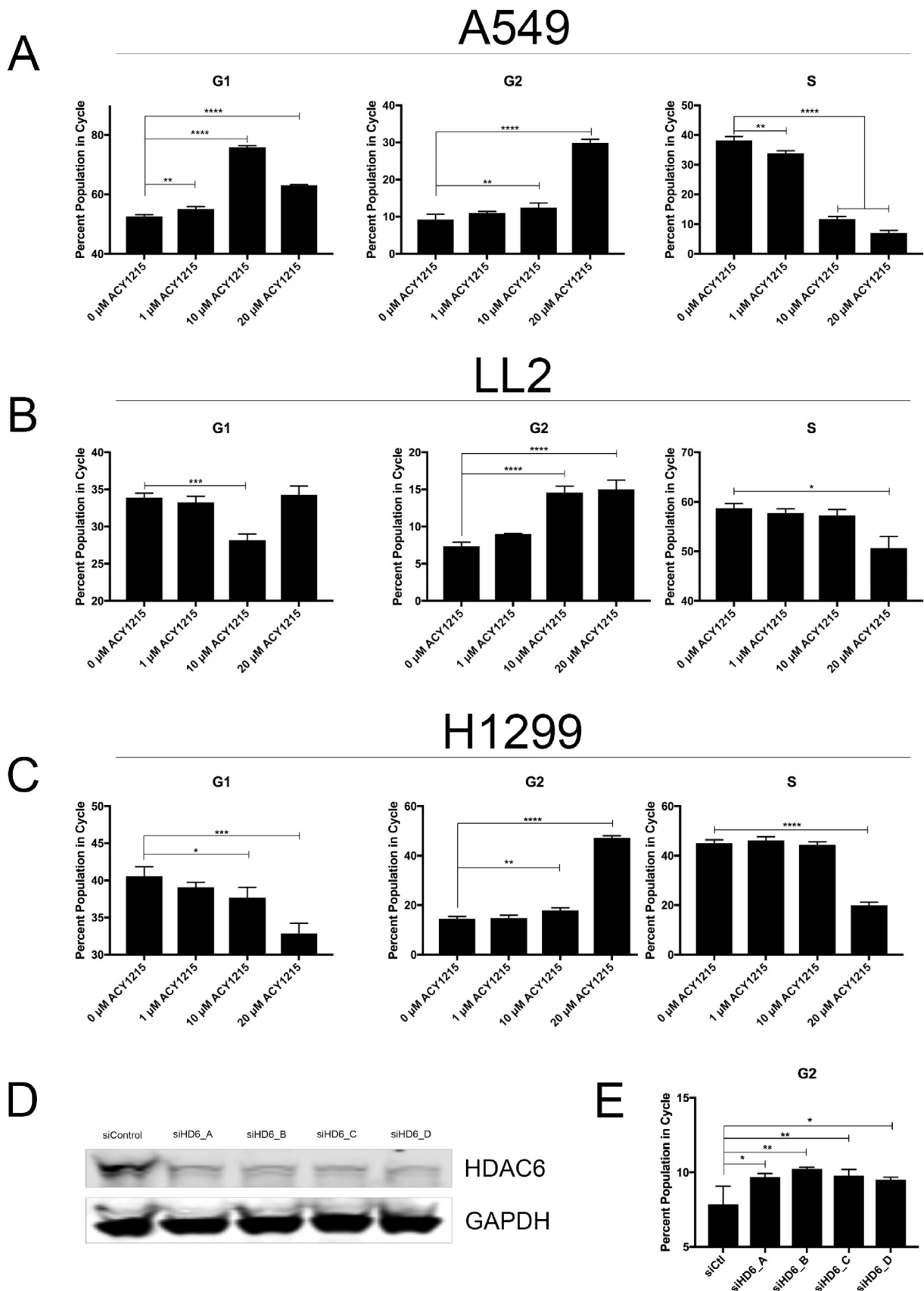


Figure 3. Cell cycle analysis of HDAC inhibition in NSCLC. (A–C) Cell cycle analysis of A549 (A), LL2 (B), and H1299 (C) cells treated with the indicated concentration of ACY1215 for 24 h. (D) Western analysis of A549 cells transfected with four separate siRNAs targeting HDAC6 (siHDAC6_A–D) or nontargeting control siRNA (siControl) for 48 h. (E) Cell cycle analysis of A549 cells treated with the same experimental conditions as in panel D. Cell cycle data presented as mean \pm STD from experimental triplicates in panels A through C and E. ANOVA test used to compare treatment groups to the DMSO control group (* $p < 0.05$; ** $p < 0.01$; *** $p < 0.001$; $p < 0.0001$).

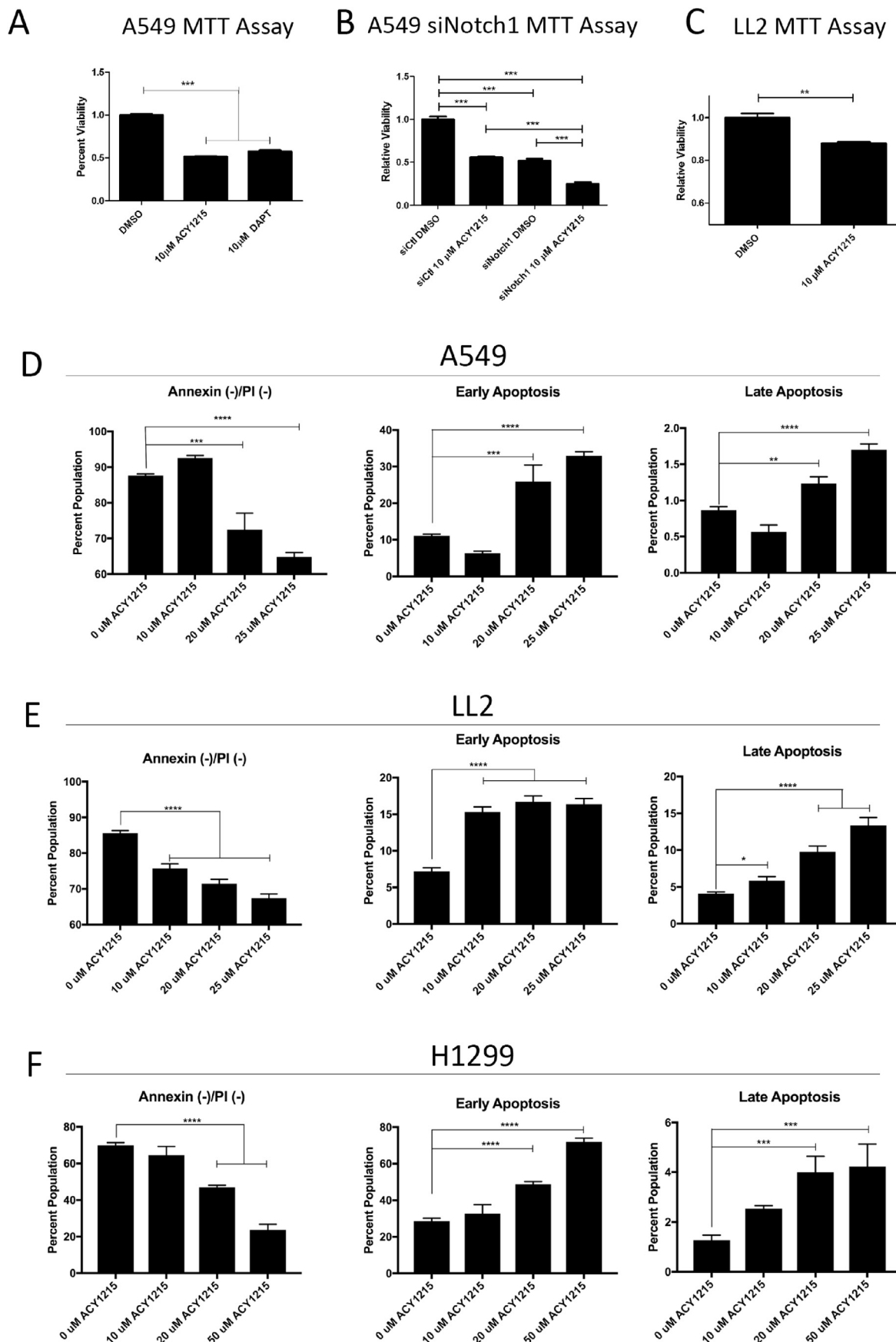


Figure 4. HDAC6 inhibition reduces cell viability in NSCLC. (A) MTT assay of A549 cells treated with the indicated concentrations of HDAC6 inhibitor ACY1215 or the γ -secretase inhibitor DAPT for 24 h. (B) MTT assay of A549 cells transiently transfected with siRNA targeting Notch1 or nonspecific control siRNA and treated with 10 μ M ACY1215. (C) MTT assay of LL2 cells treated with 10 μ M

followed by a two day period of nonadministered therapy. A 50:50 ratio of inhibitor brought up in 50 μ L DMSO (or DMSO alone for the control group), and 50 μ L $1 \times$ PBS was used to deliver the dose. ACY1215 was administered i.p. at a concentration of 50 mg/kg.

Results

HDAC6 Inhibition Reduces Notch1 Levels

Our previous work demonstrated the requirement of HDAC6 for TGF- β -induced EMT as well as TGF- β -induced Notch1 signaling in NSCLC [15,17]. We continued our investigation of HDAC6 mediation of Notch1 receptor levels using the NSCLC cell line, A549. Western blot analysis of A549 cells treated with 8 μ m tubacin for 18 h displayed significantly reduced levels of the Notch1 receptor transmembrane isoform (Figure 1A and B). We also chose to use an alternative HDAC6-selective inhibitor in our experiments, ACY1215, as it has been used in clinical investigations [18,19]. We tested whether HDAC6 inhibition with ACY1215 could recapitulate the observed loss in Notch1 receptor levels when A549 cells were treated with tubacin. We also extended our experiments to include two other NSCLC cell lines: the human derived NSCLC carcinoma H1299 cell line and the murine-derived LL2 lung carcinoma cell line. We observed a dose-dependent decrease in Notch1 receptor protein levels in response to increasing ACY1215 treatment in the A549, H1299, and LL2 cell lines indicating that a function of HDAC6 in NSCLC is to support the oncogenic Notch1 signaling circuit (Figure 1C–E).

HDAC6 Regulation of Proteasomal Degradation of the Notch1 Receptor

Our data demonstrating that HDAC6 regulates Notch1 receptor levels led us to investigate whether the Notch1 receptor is being protected from proteasomal degradation by HDAC6 functions. To test this hypothesis, we treated A549 cells with the HDAC6 inhibitor tubacin in the presence or absence of the proteasome inhibitor MG132. Inhibition of HDAC6 with 8 μ m tubacin reduced Notch1 protein levels, while cotreatment with tubacin and proteasome inhibitor MG132 rescued Notch1 levels, suggesting that HDAC6 functions to direct the Notch1 receptor away from degradation pathways (Figure 2A). To probe whether the observed degradation of the Notch1 receptor was through ubiquitin-mediated degradation, we performed immunoprecipitation of A549 cell lysates subjected to the same experimental conditions as Figure 2A (Figure 2B). Immunoprecipitation with an ubiquitin-specific antibody followed by western analysis for Notch1 revealed that HDAC6 inhibition with tubacin treatment alone reduced levels of ubiquitinated Notch1, while combined treatment with tubacin and MG132 restored ubiquitinated-Notch1 levels; HDAC6 inhibition in the presence of proteasome inhibition rescued levels of the Notch1 receptor. It is worth noting that we expected a smeared banding pattern for ubiquitinated Notch1; however, a distinct band was evident suggesting monoubiquitination versus polyubiquitination [20]. Monoubiquitination of the Notch1 transmembrane and the active, cleaved intracellular isoform (Notch-ICN) is a regulatory mechanism of the Notch signaling network with functional consequences

depending on the context specificity of the signal network [21]. These results can be interpreted in several ways: they suggest either inhibition of HDAC6 expedites monoubiquitinated Notch1 to be degraded through the UPS or that total levels of Notch1 receptor are reduced due to HDAC6 inhibition, and therefore, the ubiquitinated moiety is concomitantly reduced as there is less substrate available for ubiquitination. As a complimentary experiment, we inhibited de novo protein synthesis with cycloheximide in the presence of tubacin. When translation was inhibited with cycloheximide in the presence of HDAC6 inhibition with tubacin, Notch1 receptor levels were reduced at a significantly faster rate than the control treatment group that was treated with cycloheximide alone (Figure 2C and D). Importantly, Notch1 levels were rescued when the cycloheximide and tubacin cotreatment group was also treated with the proteasome inhibitor MG132, confirming that the Notch1 receptor was actively being degraded through the UPS (Figure 2D, Lanes H & I).

HDAC6 Inhibition Induces G2-Phase Cell Cycle Arrest

HDAC6 has been reported to play a major role in supporting progression of the cell cycle in a variety of cancers [22]. Through its α -tubulin deacetylase activities and its interaction with Aurora kinases A and B, HDAC6 supports progression through the cell cycle [22,23]. To test whether HDAC6 supports cell cycle progression in NSCLC, we used the HDAC6-selective inhibitor ACY1215 and treated cells with increasing doses in the micromolar range for 24 h. At the 10 μ m ACY1215 dose, we observed a consistent G2 arrest that increased dose dependently with 20 μ m ACY1215 across the three NSCLC cell lines tested. We also observed a concomitant drop in S-phase across the three cell lines in response to increased titration of ACY1215 (Figure 3A–C). To test the specificity of ACY1215 for HDAC6, we used four specific siRNAs to knockdown HDAC6 in the A549 cell line. Knockdown of HDAC6 significantly increased the G2-arrested population in all four of the treatment groups compared with the control group, confirming that the effect of ACY1215 is specific against HDAC6 enzymatic activity (Figure 3D and E).

Inhibition of HDAC6 Reduces Viability and Increases Expression of Apoptotic Markers in NSCLC

As a measure of cell viability, the MTT assay was employed to test the effect of treatment with ACY1215 for 24 h, on the NSCLC lines. The A549 cell line showed significant sensitivity to 10 μ m ACY1215 (Figure 4A). To test the effect of Notch1 receptor levels on cell viability, we transiently transfected A549 cells with siRNA targeting Notch1 or nonspecific siRNA and exposed the cells to 10 μ m ACY1215 for 24 h. ACY1215 treatment alone in the nonspecific siRNA group significantly reduced viability compared with the negative control siRNAs. Knockdown of Notch1 alone led to a significant reduction in viability compared with the negative control siRNA group. A combination of siNotch1 and 10 μ m ACY1215 significantly enhanced the reduction in viability compared with each treatment individually as well as the control group (Figure 4A and B). The LL2 cell line also showed a significant reduction in viability when treated with ACY1215 at 10 μ m for 24 h (Figure 4C). We observed a dose-dependent increase in the percentage of populations in early apoptosis and late apoptosis in response to ACY1215 treatment for

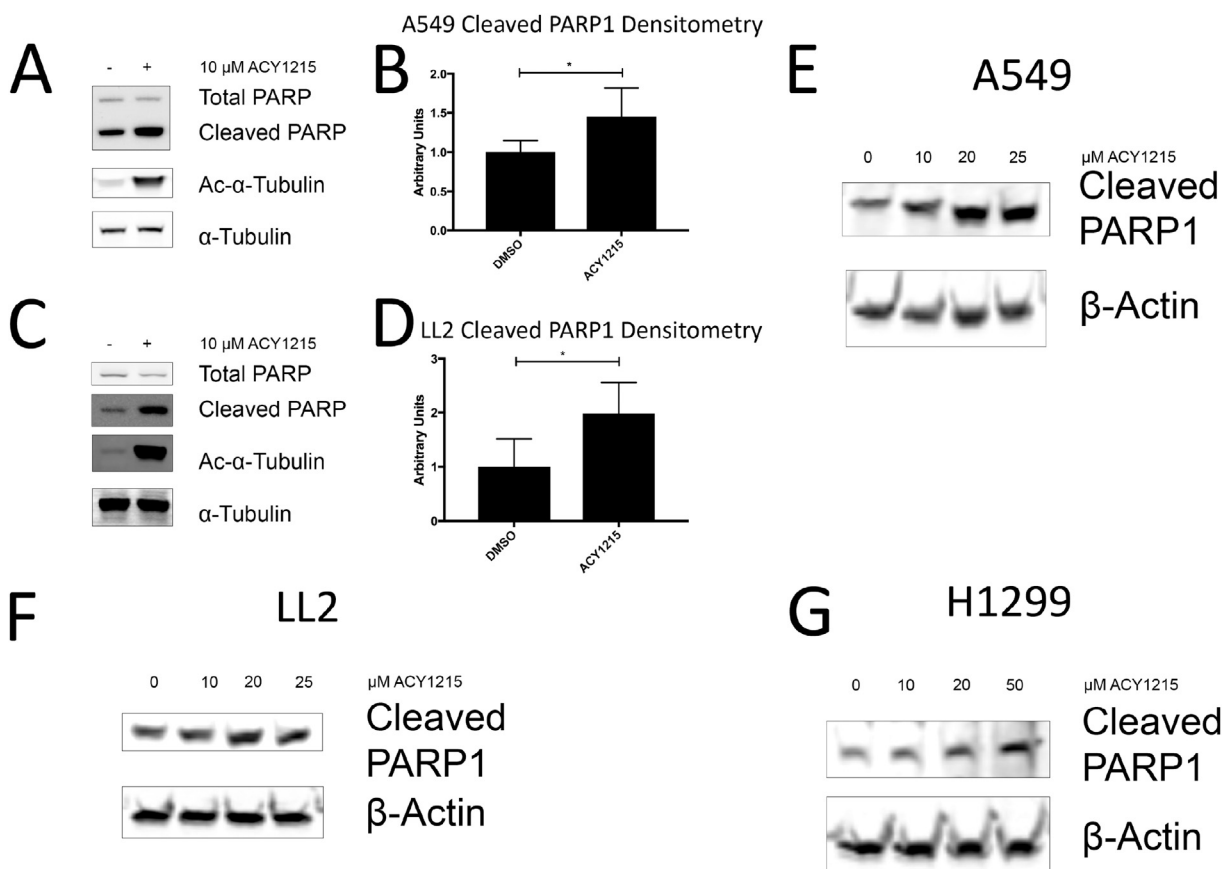


Figure 5. *In vitro* inhibition of HDAC6 enhances apoptotic markers in adenocarcinoma. (A) Western analysis of A549 cells treated with 10 μ M ACY1215 for 18 h. (B) Densitometry analysis of panel A cleaved PARP isoform presented as arbitrary units. (C) Western analysis of LL2 cells treated with 10 μ M ACY1215 for 18 h. (D) Densitometry analysis of panel C cleaved PARP isoform presented as arbitrary units. (E–G) Western analysis of PARP1 levels in A549 (E), LL2 (F), and H1299 (G) cells treated with a range of doses of ACY1215 for 24 h. Data presented as mean \pm STD of from six separate experiments using A549 cultures (Panels A and B) and four separate experiments using LL2 cultures (Panels C and D) (* $p < 0.05$).

24 h in the A549, LL2, and H1299 cell lines (Figure 4D–F). To elucidate the mechanisms of toxicity elicited by HDAC6 inhibition in these cell lines, we assayed biomarkers of apoptosis by western analysis. We found that 18 h of HDAC6 inhibition with 10 μ M ACY1215 significantly induced PARP-1 cleavage in both A549 and LL2 cells compared with the control treatment (Figure 5A–D). Furthermore, we observed a dose-dependent increase in cleaved PARP1 levels with increasing doses of ACY1215 in the A549, LL2, and H1299 cell lines. We also included blots of acetyl- α -tubulin to confirm the selectivity of ACY1215 for the HDAC6 deacetylase enzymatic functions as α -tubulin is a well-established substrate of HDAC6 (Figure 5A and C) [24].

Inhibition of HDAC6 in an In Vivo Syngeneic NSCLC Model

To evaluate HDAC6 inhibition as a strategy to target NSCLC *in vivo*, we extended our analysis to a syngeneic mouse model of NSCLC, namely the LL2 syngeneic model. In short, LL2 cells were stably transduced with a luciferase-expressing construct (LL2-Luc cells) to allow for *in vivo* monitoring of tumor progression in C57/Bl6 mice. Six days after tumor instillation with LL2-Luc cells, tumors were imaged and ACY1215 treatment was initiated (Figure 6). ACY1215 treatment was administered in 50 mg/kg doses five consecutive times a week by IP injection followed by two days of no treatment. By as early as two weeks of ACY1215 administration, a

significant decrease in relative tumor growth rate was observed in the ACY1215-treated group compared with the vehicle-treated control, and this decrease was maintained into the third week of ACY1215 treatment (Figure 6).

Discussion

Despite recent advances in targeted therapies for NSCLC patients, lung cancer remains the leading cause of cancer death worldwide [25]. Our current study investigated the mechanisms by which HDAC6 supports NSCLC through regulation of the Notch1 receptor. In our previous work, we identified HDAC6 as a requirement for Notch-ICN nuclear translocation in response to TGF- β 1 stimulation [15]. From this current set of experiments (Figures 1 and 2) and our previous work, it can be taken that inhibition of HDAC6 reduces total levels of the Notch1 receptor as well as the ubiquitinated moiety of truncated isoforms, irrespective of being marked for degradation or as a signaling event. Stated simply, HDAC6 inhibition reduces total protein levels of Notch1 through UPS-mediated degradation in NSCLC.

In vitro inhibition of HDAC6 with tubacin or ACY1215 reduces NSCLC growth rate via decreased cell proliferation and increased apoptosis through PARP1 cleavage. Our *in vitro* studies investigating the combined effect of HDAC6 inhibition with proteasome inhibition demonstrates that HDAC6 maintains Notch1 receptor

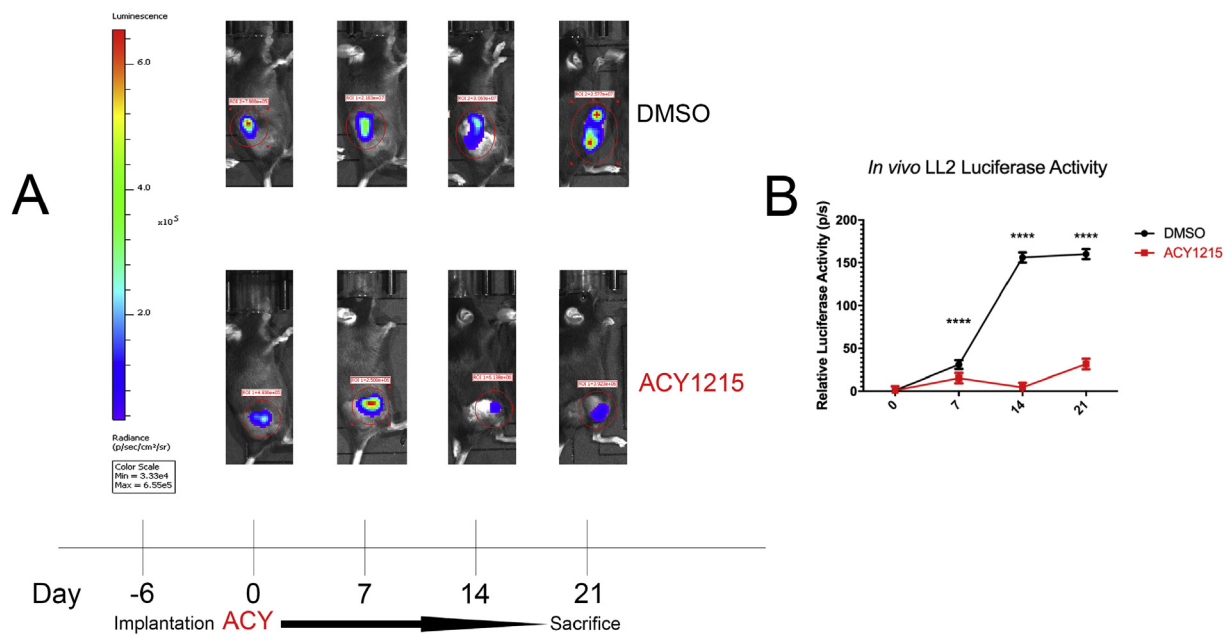


Figure 6. *In vivo* inhibition of HDAC6 reduces tumor growth rate in LL2 tumors. (A) Experimental design for *in vivo* analysis of HDAC6 inhibition on tumor growth rate; ACY indicates ACY1215 treatment. (B) Relative luciferase values of mice imaged over a three-week period (data are expressed as photons per second over a 60 s acquisition; the total luciferase activity (photons/second) was relativized to 1 at Day 0 for each treatment group). Day 6 represents the time of tumor implantation, Day 0 indicates the ACY1215 treatment began as well as the first time the tumors were imaged; Days 7, 14, and 21 are labeled to indicate the days imaging took place. n = 8 for DMSO group and n = 8 for ACY1215 Days 0 and 7 then n = 7 for Days 14 and 21. Student's *t*-tests were used to compare the normalized average means of each of the treatment groups for each measurement. Error bars presented as the standard error generated from log transformed standard deviation (***p < 0.0001).

levels by protection from proteasomal degradation (Figure 2). Our results from the *in vitro* studies provide a mechanistic rationale for HDAC6 inhibition as a therapeutic intervention for NSCLC patients. We observed that inhibition of HDAC6 with 10 μm ACY1215 reduced cell viability of both A549 and LL2 cells as measured by MTT assay as well as a dose-dependent increase in apoptosis in response to ACY1215 treatment in all three cell lines we used in this study (Figure 4 and Figure S2). Knockdown of the Notch1 receptor demonstrated a drop in viability, demonstrating the requirement of the Notch1 receptor for A549 viability; A549 viability was even further reduced when the Notch1 receptor was knocked down in the presence of ACY1215 treatment as measured by MTT assay (Figure 4B).

We also observed a delay in cell cycle progression when HDAC6 was inhibited with ACY1215. Cell cycle analysis of A549, LL2, and H1299 cells treated with increasing doses of ACY1215 for 24 h demonstrated a dose-dependent increase in G2 arrest compared with the control-treated groups. This increase in G2 arrest was accompanied by a dose-dependent drop in S-phase (Figure 3 and Figure S1). Toward addressing the specificity of ACY1215 toward HDAC6, we also performed an siRNA knockdown for 48 h using four different siRNAs targeting HDAC6. We observed a significant G2 arrest in the groups with HDAC6 knocked down compared with the siRNA control group, confirming that the observed G2 arrest induced by ACY1215 treatment was through inhibition of HDAC6 enzymatic function (Figure 3D and E). Western analysis of cell lysates of both A549 and LL2 cells treated with 10 μm ACY1215 displayed significant increases of cleaved PARP1 levels relative to controls (Figure 5A–D). We observed a dose-dependent increase in cleaved

PARP1 levels with increasing dosage of ACY1215 in the A549, LL2, and H1299 cell lines (Figure 5E–G). Taken together, HDAC6 inhibition reduced total Notch1 levels, induced cell cycle arrest, and initiated an apoptotic pathway that is marked by degradation of PARP1. The results from our *in vivo* syngeneic mouse model of NSCLC support the findings of our cell culture studies of HDAC6 inhibition. Mice bearing LL2-Luc tumors showed a significant reduction in bioluminescence evidenced within two weeks of ACY1215 treatment compared with control mice (Figure 6), demonstrating that HDAC6 inhibition with ACY1215 delayed tumorigenesis *in vivo*.

Both Notch1 and Notch3 receptor expression levels have been found to predict poor prognosis in lung adenocarcinoma patients [26]. Relative high expression of Notch1 in NSCLC adenocarcinoma patients correlates with shorter progression-free survival [26]. Mariscal et al. examined circulating tumor cells from advanced NSCLC patients by immunoisolation-based approaches followed by molecular profiling of the EpCAM-positive subfraction of cells and found that this subpopulation displayed an expression profile associated with cell adhesion, cell migration, and juxtacrine signaling pathways primarily driven by Notch1 [27]. Preclinical studies investigating the efficacy of a clinically available gamma secretase (a requisite multisubunit protein complex required for Notch signaling) inhibitor, BMS-906024, in combination with the front-line chemotherapeutic agent, paclitaxel, demonstrated increased synergy in reducing cell proliferation and enhancing apoptosis in thirty-one NSCLC cell lines, twenty-five of which were of adenocarcinoma origin [28]. A recent study investigated the use of HDAC6 inhibition with ACY1215 in combination with the bromodomain inhibitor JQ1

as a treatment strategy for NSCLC. Wong et al. sampled human peripheral blood from healthy donors and from NSCLC patients as well as NSCLC tumors and evaluated immune responses in the context of ACY1215 treatment. They found that phenotypic changes of T cells in response to ACY1215 treatment correlated with enhanced T-cell activation and an overall improvement in function in antigen-presenting cells. Treatment with ACY1215 and JQ1 in mice bearing NSCLC tumors demonstrated a synergistic effect in immune-mediated tumor growth arrest [29]. Although our study did not include analysis of the immune system in NSCLC, the authors conclude that a major effect of ACY1215 is to enhance tumor antigen presentation. We did observe a significant delay in overall LL2 tumor growth with treatment of ACY1215, and we conclude that this is because of a G2 arrest induced by HDAC6 inhibition in the tumor. Our studies support the growing body of literature that recognizes both HDAC6 and Notch signaling function to support NSCLC tumorigenesis. The novelty of this study lies in the *in vitro* demonstration of Notch signaling depending on HDAC6 activity. Herein, we provide a rationale for using ACY1215 to slow proliferation and reduce viability of NSCLC cells and provide a preclinical evaluation of drugging HDAC6 with ACY1215 using LL2 syngeneic mouse model.

In this study, we demonstrate that Notch1 receptor levels are regulated through proteasome-mediated degradation by HDAC6 function. Inhibition of HDAC6 pharmacologically induced a cell cycle arrest in the G2 phase and increased cleaved PARP1 levels in NSCLC cell lines. *In vivo* inhibition of HDAC6 with the small molecule inhibitor ACY1215 effectively reduced tumor growth rate of LL2 tumors. Our results indicate HDAC6 inhibition may be an effective therapeutic target for NSCLC, and we provide a rationale that HDAC6 functions to support Notch signaling in NSCLC. These findings warrant further pursuit to target HDAC6 as a clinical target for NSCLC patients.

Funding Sources

This study was supported by the John Deming Endowed Chair for Research and the Wetmore Foundation.

Authors' Contributions

JL and BS conceived the study. BD designed and conducted all of the experiments and analyzed the data. QY aided in the *in vivo* experiments. YZ contributed to sample preparation and some western analysis. SS aided in the analysis of the *in vivo* experiments. BD wrote the manuscript with BS and JL providing critical review. All authors reviewed, edited, and approved the final manuscript.

Conflicts of Interest

The authors have no conflicts of interest to declare. This study included vertebrate animals. The protocol and procedures were approved by Tulane University Institutional Animal Care and Use Committee.

Appendix A. Supplementary data

Supplementary data to this article can be found online at <https://doi.org/10.1016/j.tranon.2019.11.001>.

References

- [1] Siegel RL, Miller KD and Jemal A (2019). Cancer statistics. *CA: Cancer J Clin* **69**, 7–34.
- [2] Miller KD, Nogueira L, Mariotto AB, Rowland JH, Yabroff KR and Alfano CM, et al (2019). Cancer treatment and survivorship statistics. *CA: Cancer J Clin* **69**, 363–385.
- [3] Zappa C and Mousa SA (2016). Non-small cell lung cancer: current treatment and future advances. *Transl Lung Cancer Res* **5**, 288–300.
- [4] Vaughan AE, Brumwell AN, Xi Y, Gotts JE, Brownfield DG and Treutlein B, et al (2015). Lineage-negative progenitors mobilize to regenerate lung epithelium after major injury. *Nature* **517**, 621–625.
- [5] Rizzo P, Osipo C, Foreman K, Golde T, Osborne B and Miele L (2008). Rational targeting of Notch signaling in cancer. *Oncogene* **27**, 5124–5131.
- [6] Chen Y, De Marco MA, Graziani I, Gazdar AF, Strack PR and Miele L, et al (2007). Oxygen concentration determines the biological effects of NOTCH-1 signaling in adenocarcinoma of the lung. *Cancer Res* **67**, 7954–7959.
- [7] Zou B, Zhou XL, Lai SQ and Liu JC (2018). Notch signaling and non-small cell lung cancer. *Oncol Lett* **15**, 3415–3421.
- [8] de Ruijter AJ, van Gennip AH, Caron HN, Kemp S and van Kuilenburg AB (2003). Histone deacetylases (HDACs): characterization of the classical HDAC family. *Biochem J* **370**, 737–749.
- [9] Gao YS, Hubbert CC and Yao TP (2010). The microtubule-associated histone deacetylase 6 (HDAC6) regulates epidermal growth factor receptor (EGFR) endocytic trafficking and degradation. *J Biol Chem* **285**, 11219–11226.
- [10] Boyault C, Sadoul K, Pabion M and Khochbin S (2007). HDAC6, at the crossroads between cytoskeleton and cell signaling by acetylation and ubiquitination. *Oncogene* **26**, 5468–5476.
- [11] Seidel C, Schnekenburger M, Dicato M and Diederich M (2015). Histone deacetylase 6 in health and disease. *Epigenomics* **7**, 103–118.
- [12] Krämer OH, Mahboobi S and Sellmer A (2014). Drugging the HDAC6-HSP90 interplay in malignant cells. *Trends Pharmacol Sci* **35**, 501–509.
- [13] Brandvold KR and Morimoto RI (2015). The chemical biology of molecular chaperones – implications for modulation of proteostasis. *J Mol Biol* **427**, 2931–2947.
- [14] Boyault C, Zhang Y, Fritah S, Caron C, Gilquin B and Kwon SH, et al (2007). HDAC6 controls major cell response pathways to cytotoxic accumulation of protein aggregates. *Genes Dev* **21**, 2172–2181.
- [15] Deskin B, Lasky J, Zhuang Y and Shan B (2016). Requirement of HDAC6 for activation of Notch1 by TGF-beta1. *Sci Rep* **6**, 31086.
- [16] Antoon JW, Lai R, Struckhoff AP, Nitschke AM, Elliott S and Martin EC, et al (2012). Altered death receptor signaling promotes epithelial-to-mesenchymal transition and acquired chemoresistance. *Sci Rep* **2**, 539.
- [17] Shan B, Yao TP, Nguyen HT, Zhuo Y, Levy DR and Klingsberg RC, et al (2008). Requirement of HDAC6 for transforming growth factor-beta1-induced epithelial–mesenchymal transition. *J Biol Chem* **283**, 21065–21073.
- [18] Vogl DT, Raje N, Jagannath S, Richardson P, Hari P and Orlowski R, et al (2017). Ricolinostat, the first selective histone deacetylase 6 inhibitor, in combination with bortezomib and dexamethasone for relapsed or refractory multiple myeloma. *Clin Cancer Res* **23**, 3307–3315.
- [19] Yee AJ, Bensinger WI, Supko JG, Voorhees PM, Berdeja JG and Richardson PG, et al (2016). Ricolinostat plus lenalidomide, and dexamethasone in relapsed or refractory multiple myeloma: a multicentre phase 1b trial. *Lancet Oncol* **17**, 1569–1578.
- [20] Gupta-Rossi N, Six E, LeBail O, Logeat F, Chastagner P and Olry A, et al (2004). Monoubiquitination and endocytosis direct gamma-secretase cleavage of activated Notch receptor. *J Cell Biol* **166**, 73–83.
- [21] Guruharsha KG, Kankel MW and Artavanis-Tsakonas S (2012). The Notch signalling system: recent insights into the complexity of a conserved pathway. *Nat Rev Genet* **13**, 654–666.
- [22] Li T, Zhang C, Hassan S, Liu X, Song F and Chen K, et al (2018). Histone deacetylase 6 in cancer. *J Hematol Oncol* **11**, 111.
- [23] Cha TL, Chuang MJ, Wu ST, Sun GH, Chang SY and Yu DS, et al (2009). Dual degradation of aurora A and B kinases by the histone deacetylase inhibitor LBH589 induces G2-M arrest and apoptosis of renal cancer cells. *Clin Cancer Res* **15**, 840–850.
- [24] Hubbert C, Guardiola A, Shao R, Kawaguchi Y, Ito A and Nixon A, et al (2002). HDAC6 is a microtubule-associated deacetylase. *Nature* **417**, 455–458.
- [25] Torre LA, Bray F, Siegel RL, Ferlay J, Lortet-Tieulent J and Jemal A (2015). Global cancer statistics, 2012. *CA: Cancer J Clin* **65**, 87–108.

- [26] Chen CY, Chen YY, Hsieh MS, Ho CC, Chen KY and Shih JY, et al (2017). Expression of notch gene and its impact on survival of patients with resectable non-small cell lung cancer. *J Cancer* **8**, 1292–1300.
- [27] Mariscal J, Alonso-Nocelo M, Muinelo-Romay L, Barbazan J, Vieito M and Abalo A, et al (2016). Molecular profiling of circulating tumour cells identifies notch1 as a principal regulator in advanced non-small cell lung cancer. *Sci Rep* **6**, 37820.
- [28] Morgan KM, Fischer BS, Lee FY, Shah JJ, Bertino JR and Rosenfeld J, et al (2017). Gamma secretase inhibition by BMS-906024 enhances efficacy of paclitaxel in lung adenocarcinoma. *Mol Cancer Ther* **16**, 2759–2769.
- [29] Adeegbe DO, Liu Y, Lizotte PH, Kamihara Y, Aref AR and Almonte C, et al (2017). Synergistic immunostimulatory effects and therapeutic benefit of combined histone deacetylase and bromodomain inhibition in non-small cell lung cancer. *Cancer Discov* **7**, 852–867.